BEC BIOENERGETICS COMMUNICATIONS
Bioenerg Commun 2023.3
https://doi.org/10.26124/bec:2023-0003
Open Access

Technical Communication

Cite
Rodríguez E, Bettinazzi S, Inwongwan S, Camus MF, Lane N (2023) Harmonizing protocols to measure *Drosophila* respiratory function in mitochondrial preparations. Bioenerg Commun 2023.3. https://doi.org/10.26124/bec:2023-0003

Author contributions
ER, SB, SI: study design, experimental work and manuscript preparation.
FC: experimental work and manuscript preparation;
NL: manuscript preparation and funding.

Conflicts of interest
The authors declare no conflicts of interest.

Received 2023-03-12
Reviewed 2023-05-22
Revised 2023-06-14
Accepted 2023-07-19
Published 2023-08-01

Open peer review
Lisa Chakrabarti (editor)
Marcus Oliveira (reviewer)
Adam Chicco (reviewer)
Alba Timon-Gomez (reviewer)

Keywords
Drosophila;
mitochondria;
respirometry;
oxygen diffusion;
fluorescence;
reproducibility

Harmonizing protocols to measure *Drosophila* respiratory function in mitochondrial preparations

Enrique Rodríguez[1*], Stefano Bettinazzi[1], Sahutchai Inwongwan[1,2], M. Florencia Camus[1], Nick Lane[1]

[1] Research Department of Genetics, Evolution and Environment, University College London, UK
[2] Department of Biology, Faculty of Science, Chiang Mai University, Thailand

* Corresponding author: enrique.rodriguez@ucl.ac.uk

Summary

Recent advances in fluorespirometry have enabled measurements of multiple mitochondrial parameters. However, specific protocols vary widely between research groups, organisms, and tissues, sometimes without adequate justification, or based on assumptions not supported by data. This is particularly clear in *Drosophila* studies, a common model organism in biomedical research, which is increasingly popular in mitochondrial studies. We first surveyed the literature on *Drosophila* fluorespirometry to compare and contrast approaches used in the field. Then, we showed that, in contrast to assumptions based on mammalian studies, oxygen diffusion is not limited in the permeabilized thoracic muscle of this species. We further compared permeabilization and homogenization approaches, showing that the former are better in *Drosophila* thoraces. Finally, we assessed the concentration-dependent effect of various commonly used fluorescent probes on mitochondrial respiration, showing that some probes strongly affect mitochondria: care needs to be taken in the choice of concentration and probe. We recommend working towards the harmonization of protocols for assessing mitochondrial function in fruit flies.

1. Introduction

Drosophila species, and in particular *D. melanogaster,* are widely recognized and used as powerful model organisms in biological and biomedical research (Markow 2015). In the last decade, *Drosophilae* have been increasingly used to investigate the roles of mitochondria in diseases, environmental change, and evolutionary biology (Camus et al 2012; Carnegie et al 2021; Cormier et al 2019; Jørgensen et al 2021; Pichaud et al 2011; Rodríguez et al 2021; Wolff et al 2016). Since the development and increase in popularity of high-resolution fluorespirometry to analyze mitochondrial function, researchers have often sought to adapt existing protocols (often developed on murine and human models) to measure *Drosophila* mitochondrial respiration. A survey of the literature quickly shows the wide variety of methods for studying *Drosophila* using the O2k-FluoRespirometer (Oroboros Instruments, Innsbruck, Austria), but the choice of these protocols often lacks clear justification, reasoning, or adaptation to the fruit flies' fundamentally different biology. This makes it challenging for researchers new to fluorespirometry to choose the optimal sample preparation or analytical protocol for their specific questions, undermining efforts to improve reproducibility and confidence in cross-study comparisons in the field (Baker 2016).

The precision and accuracy of fluorespirometry strongly depend on sample preparation, as well as instrument parameters and choice of substrate-uncoupler-inhibitor-titration protocol (SUIT, Gnaiger 2020) . Different types of mitochondrial (mt) preparations are available to address specific study questions (Doerrier et al 2018). These are commonly: isolated mitochondria (imt), tissue homogenate (thom), permeabilized muscle fibers (pfi), and permeabilized cells (pce). These preparations differ in whether the organelle is selectively removed from the cellular environment (imt), or whether mechanical (thom) and/or chemical permeabilization is performed (pfi, pce) with the cytosol washed out (Kuznetsov et al 2008; Pesta, Gnaiger 2015), to allow the exchange of soluble molecules across the plasma membrane without damaging the mitochondrial membranes (Gnaiger et al 2020) . The choice of mitochondrial preparation comes with advantages and pitfalls which have been raised and discussed in the past for other animal models; however, *Drosophilae* have so far escaped careful scrutiny.

The first problematic issue concerns the optimal oxygen saturation for measuring mitochondrial bioenergetics in the different sample preparations. This is particularly pressing when using permeabilized tissues rather than isolated mitochondria. For instance, while many studies using *Drosophila* thorax pfi advocate the oversaturation of oxygen concentrations in the respiration chambers, others simply work at ambient oxygen levels (Correa et al 2012). Addition of exogenous oxygen is argued to overcome the potential diffusion limit of oxygen across the fibers and avoid measuring mitochondria in hypoxic or anoxic states. In a mammalian study by Pesta and Gnaiger (2012), the apparent K_m for oxygen, or c_{50}, was found to be around 40–50 µM in rat and human permeabilized tissues (soleus, heart, vastus lateralis), 100-fold above that of isolated mitochondria in ADP-stimulated respiration. The oxygen-dependence analyses of these tissues show a near hyperbolic behavior of O_2 flux, which is improved with mechanical disturbance of the fibers (*ibid*). The authors concluded that elevating oxygen concentration in the chamber was necessary in pfi to avoid hypoxic or anoxic cores in the fiber bundles, not due to the kinetics of mitochondria, but rather to the diffusion distances being much greater in these fiber bundles than in pce or imt. They recommended that chamber oxygen levels should be kept in the range of 250–500 µM when using pfi.

In flies, the thoracic flight muscle tissue is assumed to exhibit equivalent limitations in oxygen delivery (Correa et al 2012), but this was based on mammalian studies. Oxygen delivery in the insect flight muscle is critical given the high metabolic activity needed to support flight: they sustain the highest mass-specific metabolic rate of any animal, thanks in part to densely-packed mitochondria (Suarez 1998; Suarez 2000). However, to our knowledge, no study has assessed whether this limit does indeed exist. The fact that oxygen delivery to fly muscle tissue is done via tracheoles rather than capillaries might be beneficial, even more so in the context of permeabilized tissue in a respirometry chamber. Importantly, increasing O_2 concentration in the media also has potential downsides. In particular, the H_2O_2 signal depends on both the buffer and the O_2 concentration (Li Puma et al 2020). Given that a higher O_2 concentration in the chamber increases H_2O_2 flux, pfi (associated with hyperoxic conditions) is often considered to be unsuitable for the measurement of H_2O_2 flux (Oroboros-Ecosystem 2016). Experimenters have therefore generally used imt rather than pfi for fluorespirometry to overcome this limitation. Overall, establishing a reliable and shared protocol that may circumvent the hyperoxygenation issue is now an urgent priority for fluorespirometry.

This concern leads us to the second critical issue, relating to the overall reliability of the various mitochondrial preparations. Among the three major techniques (i.e. thom, pfi, imt), isolated mitochondria and permeabilized fibers are those most commonly adopted in the respirometry field (see Table 1). Using imt has potential disadvantages, as removing the organelle from its general cellular context risks stripping away critical mediators or membrane synapses that maintain mitochondrial function when working at the level of whole tissue, so long as oxygen delivery is appropriate. Tissue homogenates have also been increasingly used as a valid alternative to pfi and isolated mitochondria to study bioenergetics in a variety of tissues and species (Pecinová et al 2011; Quéméneur et al 2022; Thoral et al 2021). The advantages of this technique include fast preparation following dissection of the tissue of interest, lower perturbation of the "native" cellular environment (as opposed to imt), as well as easy access to excess sample to normalize the results by protein content or another marker of mitochondrial content (such as citrate synthase activity or mtDNA copy number), without relying on the leftover tissue retrieved from the chamber itself, which might not be accurate. Despite the potential benefits that the thom technique might have, no study has assessed the suitability of thom preparations obtained with *Drosophila* thoraces and compared their quality with more conventional pfi and imt approaches. Confidence in this preparation technique is of great importance, especially for experimental designs that are high-volume, time-consuming and costly to run.

A third important point concerns the fluorescent probes and their impact on mitochondrial respiration. The recent development of fluorescent probes for high-resolution fluorespirometry allows the combination of oxygen flux measurement with other relevant mitochondrial parameters, including H_2O_2 flux, membrane potential, rates of ATP production, and calcium flux. Nonetheless, papers using these methods on *Drosophila* flies are scarce and seldom mention method development regarding the issue of whether the probes themselves affect mitochondrial function (and if so, to what extent). Therefore, it is vital to appreciate the right chemicals and concentration for comparative and reproducibility purposes. One critical, frequently overlooked factor in mitochondrial studies is the difference in respiration or response to treatments between males and females, of concern since males remain overrepresented in animal studies (Zucker, Beery 2010). For example, our own earlier work (Camus et al 2023) has shown that female flies

are more reliant on Complex I, which makes them especially vulnerable to its suppression, potentially by fluorespirometric probes, which could impact measurements of membrane potential, ROS flux and ATP synthesis. This is not least concerning in the face of growing evidence pointing toward sex-specific diseases and dysfunctions (Morrow 2015; Ventura-Clapier et al 2017). It is clearly important to optimize protocols for both male and female tissue function, and to fully anticipate where differences might lie, or where the methodology used might obfuscate the results.

The aim of this study was to address all these questions in *Drosophila*, to give researchers better confidence in the analysis and quality of their data. First, we surveyed the O2k literature on *Drosophila* to get a sense of distribution of strains, sex, and methods used by laboratories across the world, which are reported in Table 1. We then experimentally compared rates of O_2 flux in permeabilized fibers of *Drosophila* males and females with and without oversaturation with added O_2 in the chamber, as well as with isolated thorax mitochondria, to assess whether there exists a limit to oxygen diffusion in this model. Subsequently, we compared mitochondrial preparations of pfi to thom at the levels of O_2 and H_2O_2 flux, and we finished by evaluating the effect of commonly used fluorescent probes on *Drosophila* O_2 flux.

2. Materials and methods

2.1. Literature survey of *Drosophila* studies in the O2k Respirometer

We explored the methodological sections of all the O2k-network publications stored on the "MitoPedia" (Oroboros-Ecosystem 2023) up to 01-06-2022, as well as through a Google Scholar search of "*Drosophila*" AND "Oroboros". For each study, we report the *Drosophila* species and strains used, the sex and life stage, tissue, mitochondrial preparation, respiration buffer, O2k temperature, whether additional oxygen was added to the chambers, if ROS was measured simultaneously, and the reported *RCR*s of the youngest or control flies studied (Table 1).

2.2. Fly maintenance

All *D. melanogaster* were maintained on a standard mix of molasses/cornmeal medium at a constant 25 °C on a 12/12 hour light/dark cycle, RH=50 %. 2–5 days old male and female flies from the wild type (WT) strain were used, where the $w^{1118\text{-}5095}$ nuclear genome is coevolved with the mitochondrial genome (Rodríguez et al 2021).

2.3. Preparation of fly permeabilized thoraces

Preparation of *Drosophila* permeabilized fibers (pfi) was based on a slightly modified version of Simard et al (2018). Male or female WT flies were dissected on ice in groups of three. First, head, abdomen, wings and legs were removed, and three thoraces were put in 1 mL ice-cold preservation solution (BIOPS; 2.77 mM CaK_2EGTA, 7.23 mM K_2EGTA, 5.77 mM Na_2ATP, 6.56 mM $MgCl_2$, 20 mM taurine, 15 mM Na_2phosphocreatine, 20 mM imidazole, 0.5 mM dithiothreitol, and 50 mM K-MES, pH 7.1) in a 24-well plate. Then, 80 $\mu g \cdot mL^{-1}$ saponin (5 $mg \cdot mL^{-1}$ stock solution in BIOPS) was added, shaken for 20 min on an orbital shaker, and rinsed with shaking for 5 mins in respiration buffer MiR05 (0.5 mM EGTA, 3 mM $MgCl_2 \cdot 6H_2O$, 60 mM lactobionic acid, 20 mM taurine, 10 mM KH_2PO_4, 20 mM HEPES, 110 mM D-sucrose, 1 $g \cdot L^{-1}$ bovine serum albumin, pH 7.1). The

thoraces were then carefully dry-weighed and transferred to each O2k-chamber, prefilled with 2.1 mL MiR05 respiratory buffer and kept at 25 °C. Experiments ran as explained in the corresponding sections below.

2.4. Mitochondrial isolation of fly thoraces

A total of 30 males or females of our WT strain were dissected on ice with a few drops of mitochondrial isolation buffer (250 mM sucrose, 5 mM trizma base, 2 mM EGTA, 1 % w/v bovine serum albumin, pH 7.4). Head, abdomen, wings and legs were removed and only thoraces were kept, then transferred to an Eppendorf 1.5 mL tube containing 200 µL of buffer. Thoraces were homogenized with a handheld homogenizer with a blue polypropylene pestle (100 back-and-forth passes), then filtered in a 1 mL syringe containing a small piece of gauze and transferred to another Eppendorf, with an additional 625 µL of mitochondrial isolation buffer. The homogenate was then centrifuged at 300 *g*, 4 °C for 3 minutes, filtered on gauze to a new tube as previously described, and centrifuged at 9000 *g*, 4 °C for 10 minutes. The supernatant was discarded, and the mitochondrial pellet was rinsed twice in 150 µL of isolation buffer, and finally resuspended in 60 µL of the same buffer. Protein content was then determined using the QuantiPro BCA assay kit (Sigma-Aldrich QPBCA-1KT), and mitochondrial isolate was added to a final concentration of 0.05 $mg \cdot mL^{-1}$ in the chamber.

2.5. Oxygen diffusion limit

The oxygen dependence of respiration of pfi of fly thoraces in hyperoxic (n=13) or normoxic (n=6) conditions was investigated following the trend of O_2 flux (oxygen consumption) at decreasing O_2 concentration. We used an Oxygraph-2K (Oroboros Instruments, Innsbruck, Austria) and followed the protocol established by Pesta and Gnaiger (2012). Specifically, N-pathway substrates pyruvate (P, 10 mM) and malate (M, 2 mM) were added to the chamber containing the permeabilized thoraces at air saturation. For hyperoxic conditions, pure oxygen was added up to a concentration range of 400–500 µM. Chambers were closed and LEAK-state respiration was allowed to stabilize for about 15 min, after which ADP (D, 5 mM) was added to reach phosphorylating N-linked respiration. Cytochrome *c* was added (c, 10 µM) to assess the integrity of the outer mitochondrial membrane. Runs where respiration increased over 15 % were discarded. Then, proline (Pro, 10 mM) and succinate (S, 10 mM) were added to reach maximum coupled N and S-pathway respiration, and oxygen was allowed to be consumed. During that time, O_2 flux and its linked O_2 concentration were measured at different time points, up until complete depletion of oxygen in the chambers. Then, they were reoxygenated by opening of the chambers until saturation, before closing them again and allowing the O_2 flux to stabilize. Air oxygen calibrations were performed daily, and instrumental and zero oxygen calibrations were performed at every change of MiR05 stock. All data were normalized for an internal parameter, i.e. the maximal coupled respiration achieved during the run, and expressed as flux control ratios (*FCR*, see Gnaiger et al 2020). For each run, *FCR*s were plotted as a function of oxygen concentration (Figure 2A). The best-fit curved logarithmic trendline was calculated and its equation used to extrapolate the apparent K_m for oxygen, or c_{50}, i.e. the O_2 concentration (µM) at which O_2 flux halves (*FCR* = 0.5, Figure 2B, Table S1).

2.6. Comparison of thorax permeabilized fibers and homogenates

We compared the standard thorax pfi preparation protocol (see "Preparation of fly permeabilized thoraces" section above) to various preparations of thom in WT females, using a specially designed tissue shredder (PBI-Shredder SG3, Pressure Biosciences, Medford, MA, USA) or a standard pellet pestle hand-held tissue homogenizer (Kimble Kontes Pellet Pestle Cordless Motor, DWK Life Sciences, Mainz, Germany). We followed the SUIT protocol detailed in Rodríguez et al (2021). First, measurement of H_2O_2 was possible due to the initial addition of 15 µM DTPA, 5 U·mL^{-1} SOD, 1-unit HRP, and 10 µM Amplex Ultra Red to the chamber. NADH-pathway substrates pyruvate (10 mM) and malate (2 mM) were added, followed by the pfi or thom. Chambers were closed, after which N-LEAK state (N_L) respiration was allowed to stabilize for 15 min, then ADP (5 mM) was injected to stimulate N-OXPHOS respiration (N_P), followed by proline (10 mM, $NPro_P$), succinate (10 mM, $NProS_P$), and glycerol phosphate (10 mM, $NProSGp_P$) at the end of which the maximum coupled respiration rate was reached. The uncoupler FCCP was added in 0.5 µM steps to measure maximum uncoupled respiration ($NProSGp_E$). Then, inhibitors were added: rotenone inhibiting the N-pathway (0.5 µM, $ProSGp_E$), malonate to block the S-pathway (5 mM, $ProGp_E$), and finally inhibition of Complex III was achieved with antimycin A (2.5 µM), which also allowed the estimation of residual oxygen consumption (ROX). The OXPHOS coupling efficiency (j≈*P*) with N-pathway substrates was calculated as: 1-(N_L/N_P).

2.7. Effect of fluorescent probes on respiration

All fluorophores were prepared according to the protocols published on the MitoPedia (Oroboros Instruments, Innsbruck, Austria). WT female *Drosophila* thorax pfi were prepared as described in the section above and were added to the chamber containing pyruvate (P, 10 mM) and malate (M, 2 mM). After addition of ADP (D, 5 mM) and cytochrome *c* (c, 10 µM), each fluorophore was titrated into the O2k chamber with stepwise increases in concentrations (specified in the following sections). In a parallel chamber, stepwise additions of the solvent without the fluorophore (DMSO, H_2O or ethanol) were done simultaneously. Note that cytochrome *c* was added to verify the integrity of mitochondrial preparations, but cytochrome *c* interferes with the fluorescence signal output, hence must not be used in experiments where the fluorescence signal is of particular interest (ROS flux, ATP production, membrane potential measurements, etc.).

Amplex Ultra Red: The H_2O_2 detection probe Amplex Ultra Red (AmR, Thermo Fisher A36006) was prepared at a stock solution concentration of 10 mM in fresh DMSO (https://wiki.oroboros.at/index.php/Amplex_UltraRed), and tested at concentrations ranging from 2.5 to 15 µM (a series of six 0.5 µL injections).

Magnesium Green: The probe used to measure ATP production rates, Magnesium Green (MgG, Thermo Fisher M3733), was prepared at a concentration of 1.1 mM in H_2O (https://wiki.oroboros.at/index.php/Magnesium_Green), and tested at concentrations ranging from 0.275–1.65 µM (six 0.5 µL injections).

Rhodamine 123: A 0.2 mM stock solution of membrane potential probe rhodamine 123 (Rh123, Thermo Fisher R302) was prepared in ethanol (https://wiki.oroboros.at/index.php/Rhodamine_123), and tested at concentrations ranging from 0.2 to 1.2 µM (six 2 µL injections).

Safranin: A 1 mM stock solution of membrane potential probe Safranin (Saf, Sigma S2255) was prepared in H_2O as instructed (https://wiki.oroboros.at/index.php/Safranin), and titrated at 0.5 µM increments, until a final concentration of 3.0 µM (six 1 µL injections).

TMRM: A 1 mM stock solution of membrane potential probe Tetramethyrhodamine methyl ester perchlorite (TMRM, Sigma T5428) was prepared in fresh DMSO (https://wiki.oroboros.at/index.php/TMRM), and 0.5 µM titration steps were added to the chamber until a final concentration of 3.0 µM (six 1 µL injections).

Respirometry data were normalized for a common internal parameter, the CI-sustained coupled respiration in absence of fluorescent probes (Nc_P) and expressed as flux control ratios (*FCR*). Parallel controls were titrated with an equal volume of each probe-specific solvent.

2.8. Data analysis

O2k fluorespirometry data were extracted using DatLab 7.4 software (Oroboros Instruments, Innsbruck, Austria). For the oxygen diffusion limit experiment, the comparison of c_{50} values between pfi in normoxic or hyperoxic conditions was carried out by means of a two-samples Student's *t* test. Data are presented in Table S1 as mean ± standard error of the mean (SEM). Differences in oxygen and hydrogen peroxide fluxes, dictated by the different method for sample preparation (pfi or thom) were determined through two-samples Student's *t* tests, for each parameter separately. The effect of fluorescent probe presence was inferred at each titration point by means of a two-samples *t* test. *P*-values were adjusted using Holm's correction for multiple testing. The normality and homogeneity of variance were verified with Shapiro and Levene's tests respectively. Graphics and statistical analyses were performed using MS Excel (Microsoft Corporation, 2021) and R ggplot2 package (R Team, 2016) software. Summaries are provided in Tables S1 and S2.

3. Results

3.1. A variety of approaches to assess mitochondrial function in *Drosophila*

Table 1 shows the different approaches to studying *Drosophila* mitochondrial bioenergetics in a total of 60 studies found over the last 12 years. *Drosophila melanogaster* was the preferred species in 56 out of 60 studies, with a wide variety of strains; 3 studies used *D. simulans* (Pichaud et al 2012; Pichaud et al 2011; Pichaud et al 2010), while 1 study compared six different *Drosophila* species, among which *melanogaster* (Jørgensen et al 2021). Adult flies were used in 50 papers. Males were overly represented with 25 studies, while females were found in 10 studies. Both sexes were compared in only 9 reports, while 7 did not specify the sex. Moreover, 11 papers reported using larvae but failed to report the sex (out of a total of 12 investigating the larval stage). As for tissue type, whole flies were studied 27 times, the thorax was used in 22 studies, while we could only find 2 studies on fly heads and 1 study on reproductive tissues (testes and ovaries). Mitochondrial preparations also varied, as pfi was used in 25 studies, thom in 20 and imt in 15 studies, respectively. MiR05 (the Oroboros-recommended respiration buffer) was the buffer of choice in 28 studies (including 1 using the MiR06 version), while 26 reports used one of two KCl-based buffers, and the remaining 6 used a sucrose-KCl buffer. Temperature in the O2k chambers was usually in the 24–25 °C range (45 studies),

corresponding to the rearing temperature of the flies. However, 9 studies set the O2k chamber temperature at 37 °C without apparent justification (for example, assessing mitochondrial function at higher temperatures). Out of the 25 studies on pfi, 13 increased oxygen concentration in the O2k chambers prior to the SUIT protocols. Surprisingly, two other studies increased oxygen levels, but using thom (Liu et al 2020) and imt (Cruz et al 2018), respectively. This raises the issue of hyperoxia, especially in imt, and puts the validity and comparability of the results into question. As the use of fluorescent probes to study ROS production is a relatively new addition to the Oroboros instrument, only 3 investigations reported their use simultaneously with O_2 flux analysis, all in 2021 and 2022. Finally, more than half (32/60) of the studies did not report *RCR* values, a marker of mitochondrial preparation quality (note that this parameter is being progressively replaced by the measurement of E-L coupling efficiency, see chapter 3 in Gnaiger 2020). Among the remaining 28 studies, 5 did not explicitly state *RCR*s, however these could be estimated from the figures.

Table 1. Survey of studies using *Drosophila* species in the O2k-FluoRespirometer to assess mitochondrial bioenergetics, up to 01-06-2022, showing the wide variety of approaches and methods used in the field.

Ref.	*Drosophila spp.*, strain(s)	Sex	Tissue	Mt prep.	Resp. buffer	O2k temp. (°C)	+O_2 ?	ROS	*RCR*
Guitart 2010 J Biol Chem	*D. melanogaster*, UAS and GAL	Larvae unsexed	Whole larvae	pfi	MiR05	25 and 29	No	No	4 (est.)
Pichaud 2010 J Exp Biol	*D. simulans*	Males	Thorax	imt	KCl-1	12-28 range	No	No	5 to 8
Pichaud 2011 Am J Physiol Regul Integr Comp Physiol	*D. simulans*	Females	Thorax	pfi	KCl-1	12-28 range	No	No	4 to 8
Bratic 2011 PLOS Genetics	*D. melanogaster*, UAS-RNAi lines	Adults not specified and larvae unsexed	Thorax and whole larvae	pfi	Sucrose-KCl	25	No	No	4 to 7
Stefanatos 2012 Cell Cycle	*D. melanogaster*, DAH and Ore	Adults, not specified	Whole fly	imt	KCl-1	25	No	No	N.R.
Jumbo-Lucioni 2012 BMC Genomics	*D. melanogaster* inbred DGRP strains	Males and females	Thorax	imt	KCl-1	25	No	No	10 (est.)
Correa 2012 Mitochondrion	*D. melanogaster*, Als, Dah, Jap, w1118	Males	Thorax	pfi	KCl-2:	25	Yes	No	Above 13
Pimenta De Castro 2012 Cell Death Differ	*D. melanogaster*, transgenic strains	Males	Whole fly	thom	MiR05	37	No	No	N.R.
Pichaud 2012 Evolution	*D. simulans*	Males	Thorax	pfi	KCl-1	24	No	No	5

Costa 2013 Cell Death Dis	*D. melanogaster*, transgenic strains	Males	Whole fly	thom	MiR05	37	No	No	6 (est.)
Wredenberg 2013 PLoS Genet	*D. melanogaster*, transgenic strains	Larvae unsexed	Whole larvae	pfi	Sucrose-KCl	25	No	No	4 to 7
De Castro IP 2013 Cell Death Dis	*D. melanogaster*, transgenic strains	Adults, not specified	Whole fly	thom	MiR05	37	No	No	N.R.
Macchi 2013 J Cell Sci	*D. melanogaster*, transgenic strains	Adults, not specified	Whole fly	thom	MiR05	37	No	No	N.R.
Guitart 2013 Nucleic Acids Res	*D. melanogaster*, UAS and GAL	Larvae unsexed	Whole larvae	pfi	MiR05	25 and 29	No	No	4
Pichaud 2013 Mitochondrion	*D. melanogaster*, Jap and Als	Males	Thorax	pfi	KCl-2:	23	Yes	No	Above 10
Baggio 2014 Nucleic Acids Res	*D. melanogaster*, UAS-RNAi lines	Males and females	Thorax and whole larvae	pfi	Sucrose-KCl	28	No	No	N.R.
Tufi 2014 Nat Cell Biol	*D. melanogaster*, UAS-RNAi lines	Males	Whole fly and head	thom	MiR05	37	No	No	N.R.
Kemppainen 2014 Hum Mol Genet	*D. melanogaster*, transgenic strains	Larvae unsexed, adult males and females	Whole fly	thom	KCl-1	25	No	No	N.R.
Bratic 2015 Nat Commun	*D. melanogaster*, RNAi lines	Larvae unsexed	Whole larvae	imt	MiR05	27	No	No	N.R.
Rovenko 2015 Comp Biochem Physiol A Mol Integr Physiol	*D. melanogaster*, Canton S	Males and females	Whole fly	thom	KCl-1	25	No	No	N.R.
Senyilmaz 2015 Nature	*D. melanogaster*, transgenic strains	Females	Whole larvae	pfi	MiR05	25	Yes	No	4 (est.)
Syrjanen 2015 Front Zool	*D. melanogaster*, RNAi lines	Males and females	Whole fly	thom	KCl-1	25	No	No	N.R.
Wolff 2016 J Evol Biol	*D. melanogaster*, mitonuclear strains	Males and females	Thorax	pfi	KCl-2:	25	Yes	No	N.R.
Scialò 2016 Cell Metab	*D. melanogaster*, Dah transgenic	Females	Whole fly	thom	KCl-1	25	No	No	N.R.
Scialò 2016 PLOS ONE	*D. melanogaster*, Dah transgenic	Females	Whole fly	thom	KCl-1	25	No	No	N.R.
Bratic 2016 PLoS Genet	*D. melanogaster*, UAS-RNAi lines	Larvae unsexed	Whole larvae	pfi	Sucrose-KCl	25	No	No	N.R.
Brandt 2017 eLife	*D. melanogaster*, Dah	Females	Whole fly	imt	Sucrose-KCl	37	No	No	N.R.
De Carvalho 2017 Toxicol Research	*D. melanogaster*, Harwich strain	Males and females	Whole fly	imt	MiR05	24	No	No	11 to 16

Lehmann 2017 Biology Open	*D. melanogaster*, various strains	Males	Whole fly	thom	MiR05	37	No	No	N.R.
Rana 2017 Nat Commun	*D. melanogaster*, UAS-RNAi lines	Females	Head and thorax	pfi	MiR05	25	Yes	No	N.R.
Ederer 2018 Int J Mol Sci	*D. melanogaster* inbred DGRP strains	Males	Whole fly	imt	KCl-1	25	No	No	N.R.
Rodrigues 2018 Free Radic Biol Med	*D. melanogaster*, Ore	Females	Whole fly	imt	MiR05	24	No	No	12
Cruz 2018 Chem Biol Interact	*D. melanogaster*, Harwich strain	Adults, not specified	Whole fly	Iit	KCl-1	25	Yes	No	22
Rodrigues 2018 Sci Rep	*D. melanogaster*, UAS-RNAi lines	Larvae unsexed	Whole larvae	thom	KCl-1	25	No	No	N.R.
Champigny 2018 Mar Drugs	*D. melanogaster*, w1118	Males	Thorax	pfi	KCl-1	24	Yes	No	15 to 35
Thompson 2018 EMBO Mol Med	*D. melanogaster*, UAS-RNAi lines	Males	Whole fly	thom	KCl-1	25	No	No	N.R.
Weisz 2018 Hum Mol Genet	*D. melanogaster*, various strains	Males	Thorax	imt	MiR05	25	No	No	N.R.
Simard 2018 J Vis Exp	*D. melanogaster*, various strains	Males	Thorax	pfi	KCl-1	25	Yes	No	6 to 33.55
Andreazza 2019 Nat Commun	*D. melanogaster*, various strains	Males	Whole fly	thom	Sucrose-KCl	30	No	No	N.R.
Pajak 2019 PLoS Genet	*D. melanogaster*, UAS-RNAi lines	Larvae unsexed	Whole larvae	pfi	MiR05	25	No	No	N.R.
Gururaja Rao 2019 Cells	*D. melanogaster*, various strains	Adults, not specified	Whole fly	imt	MiR05	25	No	No	N.R.
Pichaud 2019 Front Genet	*D. melanogaster* Ore and Aut, D. simulans simw501	Females	Thorax	pfi	KCl-2:	24	Yes	No	Above 10
Liu 2019 J Ethnopharmacol	*D. melanogaster*, PINK1 mutant	Males	Whole fly	thom	MiR05	37	Yes	No	N.R.
Cormier 2019 Sci Rep	*D. melanogaster*, w1118	Males	Thorax	pfi	KCl-1	24	Yes	No	10 to 20
Garrido-Maraver 2019 Cell Death Dis.	*D. melanogaster*, various strains	Males	Whole fly	thom	MiR05	37	No	No	5 (est.)
Ulgherait 2020 Nat Commun	*D. melanogaster*, various strains	Males	Whole fly	imt	MiR05	25	No	No	N.R.
Simard 2020 Metabolites	*D. melanogaster*, w1118	Males	Thorax	pfi	KCl-2:	24	Yes	No	Above 10
Simard 2020b Metabolites	*D. melanogaster*, w1118	Males	Thorax	pfi	KCl-2:	24	Yes	No	Above 10

Maddison 2020 PLoS Genet	*D. melanogaster*, various strains	Males	Whole fly	thom	MiR05	25	No	No	N.R.
Kanellopoulos 2020 Cell	*D. melanogaster*, UAS and GAL	Males	Head and body	thom	MiR06	25	No	No	N.R.
Cormier 2021 Insect Biochem Mol Biol	*D. melanogaster*, w1118	Males	Whole fly	imt	KCl-2:	24	No	No	Above 10
Wall 2021 Dis Model Mech	*D. melanogaster*, transgenic strains	Males and females	Thorax	pfi	MiR05	25	Yes	No	1 to 2
Jørgensen 2021 J Exp Biol	*Drosophila*, six different species	Females	Thorax	pfi	KCl-1	19-46 range	Yes	No	10
Rodriguez 2021 Front Genet	*D. melanogaster*, mitonuclear strains	Larvae unsexed	Whole larvae	pfi	MiR05	25	No	Yes	6 to 15
Winwood-Smith 2021 Thesis	*D. melanogaster*, wild Australian strains	Females	Thorax	Imt	MiR05	25	No	Yes	N.R.
Ebanks 2021 J Mol Sci	*D. melanogaster*, w1118	Males	Whole fly	thom	MiR05	20	No	No	N.R.
Schober 2022 Hum Mol Genet	*D. melanogaster*, Dah transgenic	Larvae unsexed	Whole larvae	pfi	MiR05	25	No	No	N.R.
Ziech 2022 Drug Chem Tox	*D. melanogaster*, Harwich strain	Adults, not specified	Whole fly	imt	MiR05	24	No	No	N.R.
Menail 2022 Front Phys	*D. melanogaster*, w1118	Males	Thorax	pfi	KCl-1	6-45 range	No	No	Above 10
Camus 2023 Exp Gerontol	*D. melanogaster*, mitonuclear strains	Males and females	Thorax and reproductive	pfi and thom	MiR05	25	No	Yes	20 (thorax); 6 (testes and ovaries)

Mitochondrial (mt) preparations: pfi = permeabilized fibers, thom = homogenates, imt = isolated mitochondria. Respiration buffer composition: MiR05 = 110 mM Sucrose, 60 mM Lactobionic acid, 20 mM Taurine, 20 mM HEPES, 10 mM KH_2PO_4, 3 mM $MgCl_2$, 0.5 mM EGTA, 1 % BSA, pH 7.1; MiR06 = MiR05 + Catalase; Sucrose-KCl = 120 mM Sucrose, 50 mM KCl, 20 mM Tris-HCl, 4 mM KH_2PO_4, 2 mM $MgCl_2$, 1 mM EGTA, pH 7.2; KCl-1 = 120 mM KCl, 5 mM KH_2PO_4, 3 mM HEPES, 1 mM EGTA, 1 mM $MgCl_2$, 0.2 % BSA, pH 7.2; KCl-2: 115 mM KCl, 10 mM KH_2PO_4, 2 mM $MgCl_2$, 3 mM HEPES, 1 mM EGTA, 0.2 % BSA, pH 7.2. *RCR*: est. = estimated from LEAK to OXPHOS respiration reported in graphical form in the paper; N.R. = not reported.

3.2. No evidence for oxygen diffusion limit in *Drosophila melanogaster* thorax tissue

The behavior of the oxygen-dependent O_2 flux showed that it was indistinguishable from isolated mitochondria of the same tissue and species. This is illustrated in Figure 1 panels A-D, where the rapid decrease in the red O_2 flux trace happens suddenly and at low O_2 concentrations. This was observed in all treatments: hyperoxic (Figure 1A, B) and normoxic O_2 (Figure 1C) concentrations for thorax pfi in both sexes, as well as for imt (Figure 1D). Figure 2A shows O_2 flux normalized as flux control ratio (*FCR*, where maximum coupled respiration is set as = 1) as a function of O_2 concentration, in two representative normoxic and hyperoxic experiments (the same as Figure 1A and C). We observe a nearly identical behavior of the two curves, showing almost no dependence of O_2 flux on O_2 concentration, until a very low level of O_2 is reached in the chamber. We then compared the apparent K_m for oxygen, or c_{50}, between normoxia and hyperoxia. For each

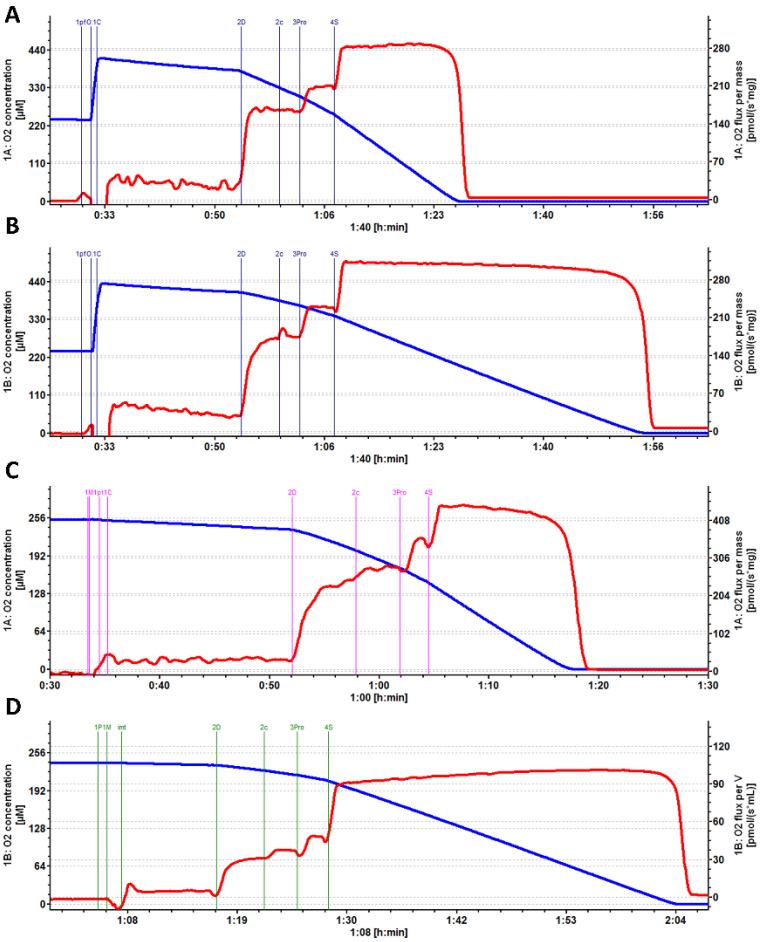

Figure 1. Representative oxygraph traces of *Drosophila* pfi respiration for female **(A)**, male **(B)** with addition of pure oxygen to the chamber (indicated by the increase in the blue oxygen concentration at the start of the experiment), and female with normal saturation of oxygen **(C)** versus isolated mitochondria (imt, **D)**. DatLab files of experiments "7-09-2021 P1-02 WT F vs M.DLD" (A and B), and "22-10-2021 P1-01 WT F pfi vs WT F Imt.DLD" (C and D). Numbered events on the traces correspond to the sequential addition of pfi, imt, substrates (P: pyruvate, M: malate, Pro: proline, S: succinate), ADP (D), cytochrome *c* (c), and closing of the chambers (C). See methods for detailed SUIT protocols.

experiment, we extracted the equation of the curve to obtain the c_{50} value for normoxic (n = 6) and hyperoxic conditions (n = 12) in males and females (details in Table S1). We found no impact of sex on the results; therefore, we combined the analysis of the results for males and females. Figure 2B shows the c_{50} values for pfi treated at normoxic (c_{50} = 0.38±0.07) and hyperoxic conditions (c_{50} = 0.82±0.08) in males and females. Although a two-sample t test showed a significant difference between the two treatments (p = 0.002), both values represent extremely low levels of oxygen in the chamber and are likely not biologically relevant (see Discussion).

3.3. Thorax homogenates are not a suitable alternative to permeabilized fibers

Thoracic tissue preparations thom and pfi differed markedly in various mitochondrial respiration parameters (Figure 3). O_2 flux was significantly reduced in tissue homogenates (thom) compared with permeabilized fibers (pfi) in WT flies. Compared to pfi, thom preparations had lower respiration rates in the N_P state: J_{O_2} (thom) = 58.22 (±8.57) pmol $O_2 \cdot s^{-1} \cdot mg^{-1}$, versus J_{O_2} (pfi) = 138.52 (±46.83) pmol $O_2 \cdot s^{-1} \cdot mg^{-1}$ (p = 0.002, Figure 3A). Coupling efficiency with N-linked substrates pyruvate and malate was also reduced in thom: j≈P_{thom} = 0.73 (±0.02), compared to j≈P_{pfi} = 0.88 (±0.03) (p = 0.008, Figure 3B); and the cytochrome *c* effect was higher in homogenates, indicating outer mitochondrial membrane damage: increase in J_{O_2} after cyt *c* addition was of 21 % (±6.42) in thom, compared to 0.51 % (±0.51) in pfi (p = 0.01, Figure 3C). Finally, H_2O_2 flux was 10 to 20-fold higher in thom than pfi for all respiratory states. In pfi, it ranged from 0.06 (±0.02) to

0.39 (±0.07) pmol $H_2O_2 \cdot s^{-1} \cdot mg^{-1}$ in N-linked coupled state (N_P) and maximum inhibition (ROX) respectively, while in thom it ranged from 0.97 (±0.05) to 3.85 (±0.34) pmol $H_2O_2 \cdot s^{-1} \cdot mg^{-1}$ in the two aforementioned states ($p \leq 0.01$, Figure 3D).

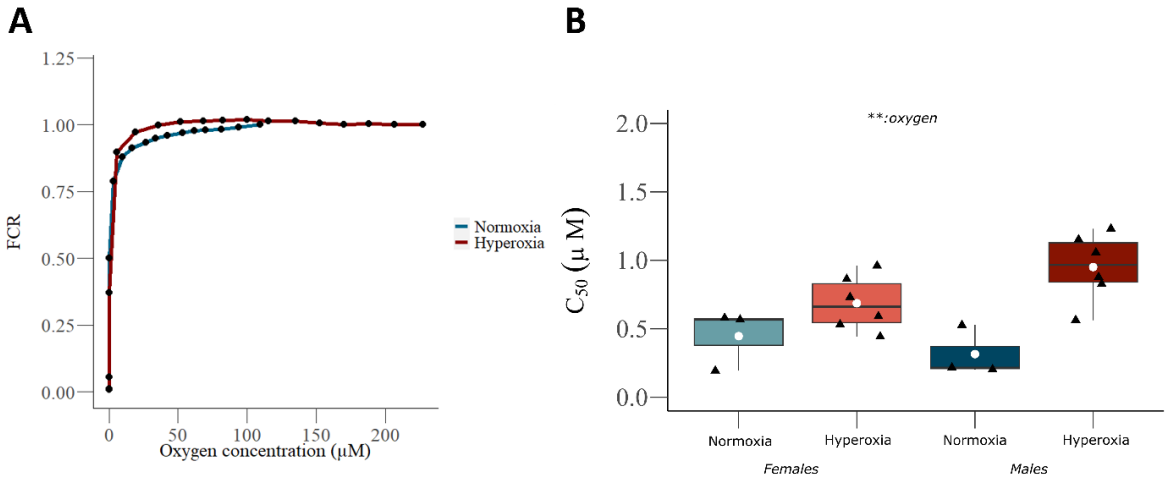

Figure 2. (A) O_2 flux presented as normalised flux control ratios (*FCR*) as a function of chamber O_2 concentration for pfi in normoxic and hyperoxic conditions (normal and high O_2). Curves are taken to two experiments: female normoxic (chamber A in "22-10-2021 P1-01 WT F pfi vs WT F Imt.DLD") and female hyperoxic (chamber A in "7-09-2021 P1-02 WT F vs M.DLD") and correspond to the traces shown in Figure 1C and 1A, respectively. **(B)** Calculated c_{50} of O_2 concentration-dependent O_2 flux for pfi in normoxic and hyperoxic conditions. Boxplots show median of runs (N = 3 for each sex in normoxia, N = 6 for each sex in hyperoxia), 25th and 75th percentiles, interquartile range and individual runs. Asterisks show a main effect of oxygen concentration (**$p \leq 0.01$; see Table S1).

3.4. Concentration-dependent effect of fluorescent probes

We compared the effect of titrating the fluorescent probes and their carrier solvent on N-linked respiration in the coupled state, after cytochrome *c* addition (Nc_P) and expressed as *FCR*s (Figure 4, Table S2). AmR exerted a significant (p = 0.05) effect at 12.5 and 15 μM when compared to the carrier solvent (DMSO), where an 18–20 % inhibition of O_2 flux was found: *FCR* = 0.93 (±0.03) for DMSO versus 0.733 (±0.03) with AmR. MgG effect did not significantly differ from the effect of the carrier H_2O: at the highest concentration (1.65 μM), *FCR* = 0.92 (±0.003) compared to 0.88 (±0.03) with MgG (p = 0.22). Rh123 exerted a significant effect on N-linked respiration compared to ethanol. Even at the mid-range concentration of 0.6 μM, it exerted a 13 % inhibition compared to ethanol: *FCR* = 0.94 (±0.02) compared to 0.81 (±0.01) with the probe (p = 0.007). The effect of Safranin was particularly strong after 1.5 μM. At the recommended final concentration of 2.0 μM, a 13 % inhibition was found, albeit not significant. Inhibition was of 30 % and significant (p = 0.006) at 2.5 μM: *FCR* = 0.97 (±0.03) with H_2O, compared to 0.67 (±0.02) with Saf. Finally, TMRM had a significant effect on respiration at every titration step, compared to DMSO: even at the second-lowest recommended concentration of 1 μM, it exerted a significant inhibition of 11 % (p = 0.04), *FCR* = 0.98 (±0.02) for DMSO versus 0.86 (±0.02) for TMRM. For the detailed results see Table S2.

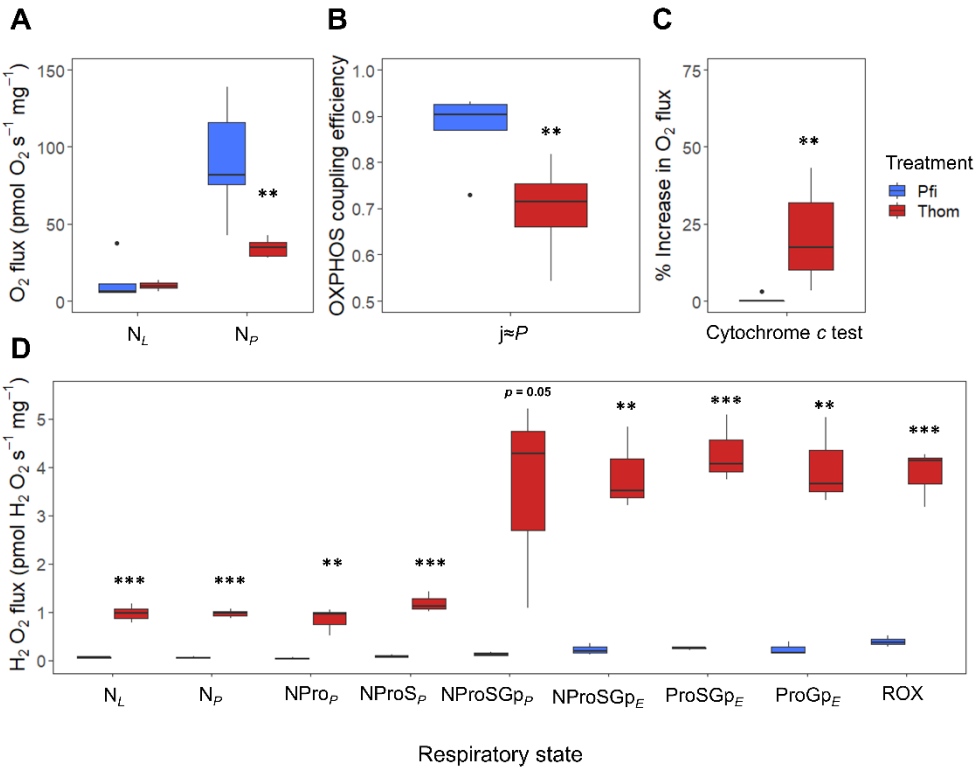

Figure 3. Fluorespirometry of permeabilized fibres (blue plots) versus tissue homogenates (red plots) in *D. melanogaster* thoraces. (A) LEAK and OXPHOS state: O_2 flux is normalised by mg wet tissue in the LEAK (N_L) and OXPHOS (N_P) states, fuelled with Complex I substrates (N-pathway). **(B)** OXPHOS coupling efficiency (j≈*P*) with N-pathway substrates **(C)** Mitochondrial membrane damage test through cytochrome *c* addition. **(D)** H_2O_2 flux in different respiratory states. Acronyms show substrates used: proline (Pro), succinate (S) and glycerophosphate (Gp); and states: ET capacity or maximum uncoupled respiration (*E*), residual oxygen consumption (ROX, after inhibition of Complexes I, II and III). Boxplots depict median values for each treatment (pfi or thom), 25th and 75th percentiles, interquartile range and outliers. Replicates per treatment: *N* = 5 for panels (A-B); *N* = 6 for panel (C); *N* = 3 for panel (D). Asterisks show significant differences (**p* ≤ 0.05, ***p* ≤ 0.01, ****p* ≤ 0.001; two-sample *t* tests) between treatments.

4. Discussion

The variety of approaches to studying *Drosophila* mitochondrial function in the circa 60 studies surveyed over a 12-year period calls for a more careful consideration of the methodological approach tailored to the research questions. Investigators need to think about the suitability of their high-resolution respirometry approach, and not merely adopt previous protocols, where parameters such as chamber temperature might be unsuitable for their study model (e.g. in studies conducted at 37 °C in mammals, and at the same temperature in flies). The purpose of this report is to help investigators choose the best conditions for their mitochondrial function analyses, warning about potential

pitfalls and limitations. For example, adding extra oxygen to isolated mitochondria or homogenates can be problematic for interpreting results in light of ROS management (Li Puma et al 2020; Munro, Treberg 2017; Treberg 2021), and might reflect how mitochondria from different fly lines or treatment react to hyperoxic conditions, rather than reflecting *in vivo* function. Moreover, analyzing mitochondrial function at higher temperatures than the flies' rearing conditions might not test standard mitochondrial function, but rather heat resistance, and this might not be the question central to the study. Assessment of the quality of mitochondrial preparations is critical for all studies, and where cytochrome *c* tests cannot be done in every run (for example, if they interfere with fluorescence signals), *RCR* and/or *P-L* control efficiency (Gnaiger 2020) values should be reported for the sake of transparency and comparison with previous studies. Finally, the male bias of *Drosophila* studies confirms what many researchers have been warning about – sex discrepancy in biomedical research. Although we recognize that it is sometimes difficult to separate males from females (for example, at the larval stages, in particular disease models, or due to time and budget constraints), we encourage investigators to study and compare both sexes where possible. In our own work, we have found important differences between the sexes in response to treatments in adults (Camus et al 2023), although we were not able to separate the sexes in our larval experiments (Rodríguez et al 2021).

We report a negligible oxygen dependence of respiration in permeabilized fibers from *Drosophila* thorax, with a 50 % decrease in respiration rate occurring at oxygen levels below 1 μM both in initial experimental normoxic or hyperoxic conditions, in females and males (Figure 2B, Table S1). Although we found a difference in the apparent K_m for oxygen (or c_{50} value) between hyperoxia and normoxia, both were between 50 and 100-fold lower than the 50 μM result reported by Pesta and Gnaiger (2012) for permeabilized fibers from human *v. lateralis* for ADP-stimulated respiration (with similar values for rat soleus and heart). A near-hyperbolic oxygen dependence of respiration was apparent in the mammalian study, while our results in flies showed no differences in the behavior of the oxygen flux traces at low concentrations (Figure 1 and 2A) – almost indistinguishable from isolated mitochondria from *Drosophila* thorax. Hence, despite more than half of the studies on this tissue and species (Table 1), we conclude that it is not necessary to increase the amount of oxygen in the O2k-chamber before measuring mitochondrial respiration in *Drosophila* thorax pfi. In fact, it is likely that these hyperoxic conditions do not represent the physiological functioning of flight muscle in flies and might impact ROS balance by increasing rates of production. We therefore recommend that future studies do not hyperoxygenate at the start of a SUIT protocol in thorax pfi, as respiration will remain stable at very low levels of oxygen. We suspect that this finding applies to the flight muscle of other flying insects, but researchers are encouraged to validate this by following the protocols outlined here.

A crucial step when measuring mitochondrial function is tissue preparation, as this will impact the quality and reproducibility of the data. An ideal tissue preparation must be as fast, reproducible and as physiologically relevant as possible to address the questions studied. We report that the use of tissue homogenates of *Drosophila* thorax might not be appropriate with two types of homogenizers: the PBI-Shredder, and the handheld pellet pestle homogenizer. Both approaches yielded less coupled, more damaged mitochondria with lower rates of respiration, and much higher rates of H_2O_2 efflux (Figure 3). The PBI-Shredder has to our knowledge only been successfully used on mice and fish heart, brain and liver tissues (Doerrier et al 2015; Eigentler et al 2015). The

use of *Drosophila* thom, with the two homogenizers tested in this study, is therefore not recommended. Other softer means of preparing thom might be considered; indeed, a soft Dounce homogenizer, where a specific rotation speed can be chosen, reportedly yields good quality thom mitochondrial preparation (Dr. Brian Irving, *personal communication*). Another method also worth considering relies on the permeabilization of the thoraces directly in the O2k-chamber with higher stirring speeds without the need for chemical agents, and appears to give well coupled and reproducible results (Gaviraghi et al 2021).We find that gentle homogenization of reproductive tissue (testes and ovaries) yields adequate results in *Drosophila*, contrary to the thorax (Camus et al 2023). Therefore, researchers need to carefully consider their tissue and mt-preparation of choice, test and compare their values for O_2 flux, coupling, cytochrome *c* tests and H_2O_2 efflux with previously published results.

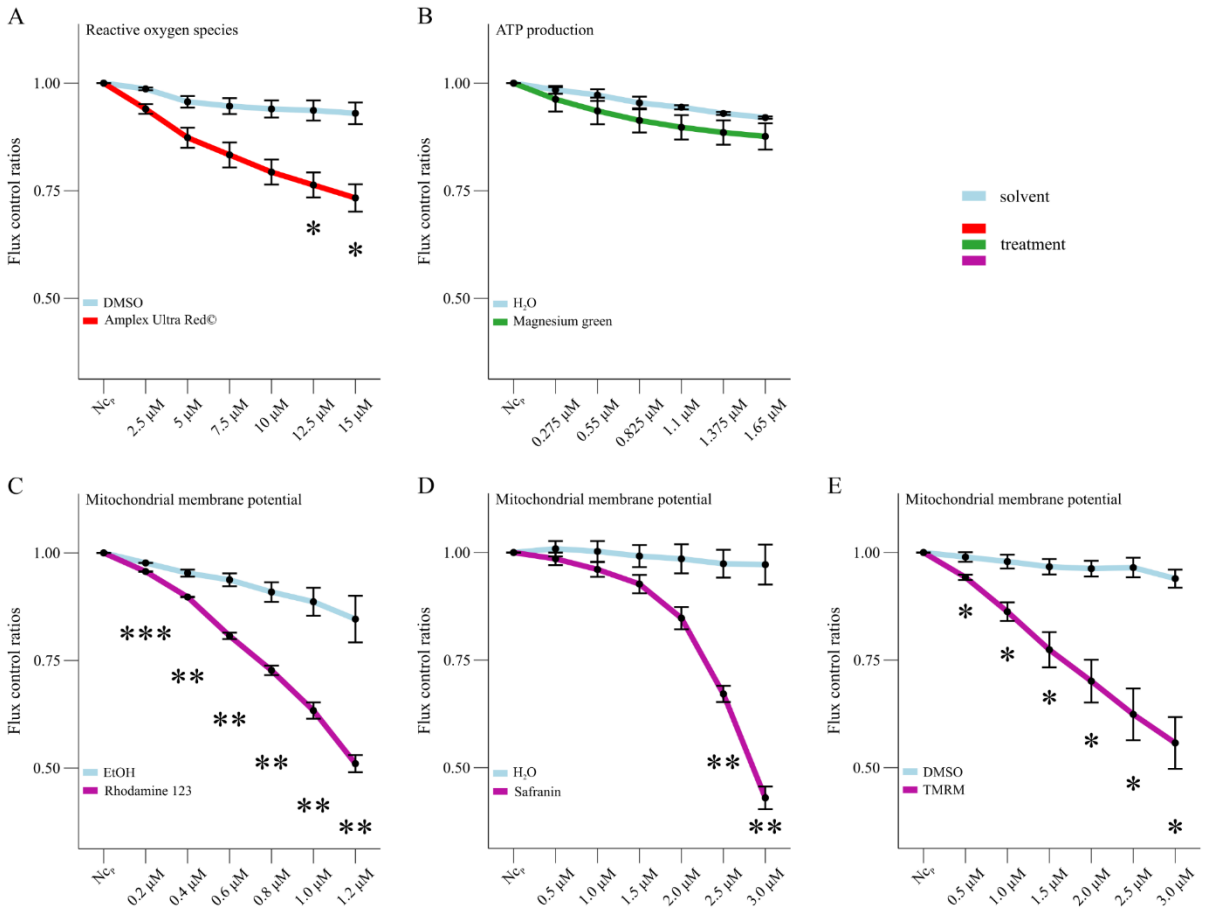

Figure 4. Effect of various fluorescent probes on N-pathway linked respiration in *Drosophila* thoraces pfi. (A) Amplex Ultra Red titration compared to the carrier DMSO. **(B)** Magnesium Green compared to water. **(C)** Rhodamine 123 compared to ethanol. **(D)** Safranin versus water. **(E)** TMRM compared to DMSO. Data are presented as means of */N* = 6 experiments for each probe. The effect of probe presence was inferred at each titration point by means of a two-samples *t* test. *p*-values were adjusted using Holm's correction for multiple testing: **p* ≤ 0.05; ***p* ≤ 0.01; ****p* ≤ 0.001.

The development of fluorescent probes to study various mitochondrial parameters has multiplied over the last decades, with these applications reaching the O2k-FluoRespirometer environment more recently with the introduction of the Fluo-Sensors (Gnaiger et al 2021). These applications are not yet widespread to the *Drosophila* mitochondrial field, therefore we sought to evaluate their applicability. We titrated some of the most commonly used fluorescent agents to test their concentration-dependent effects on respiration in *Drosophila* thorax (Figure 4, Table S2). While the ATP production probe Magnesium Green (MgG) exerted no significant effect on N-linked respiration (as previously reported by Cardoso et al 2021), we found strong inhibitory effects of mitochondrial membrane potential probes Rhodamine 123 (Rh123), Safranin (Saf) and Tetramethyrhodamine methyl ester perchlorite (TMRM), as well as a moderate effect of the H_2O_2 detector Amplex Ultra Red (AmR). The concentrations recommended by the manufacturer of the O2k-FluoRespirometer vary depending on the specific probe. At 10 µM AmR, the inhibition of around 15 % was not significantly distinguishable from the effect of the carrier (DMSO), and therefore appears acceptable for measurements. At the suggested range of 0.2–1 µM for Rh123, the inhibition was significantly higher than for the carrier (EtOH) and reached over 25 % N-pathway inhibition after 0.5 µM. Safranin strongly inhibited N-linked respiration at 2.5 µM (above the 2.0 µM suggested concentration, which still showed a 15 % inhibition of respiration). TMRM is recommended to be used at 0.5–2 µM, and all these concentrations significantly inhibited respiration compared with the carrier DMSO, although the lower range might be suitable and comparable to Safranin and AmR (around 15 % inhibitory effect). Therefore, we recommend careful consideration and fine-tuning of the concentration before use by researchers wanting to assess these parameters. For example, experiments could be run at the lower concentration end of quenching mode, but the intensity of fluorescence can be increased to be able to obtain a good signal to noise ratio. It appears difficult to avoid a certain degree of inhibition with the currently available probes on the market, but it is important for researchers to be aware of this and to work with concentrations that minimize these effects. More research needs to be done on the development of better reporter probes to assess all types of mitochondrial parameters.

Research in the biological and biomedical fields is currently facing a reproducibility crisis (Baker 2016; Gnaiger 2019). One way to address and attempt to solve this crisis involves being more thoughtful and transparent when choosing methodological approaches and harmonizing these techniques where possible. We hope that our study will give researchers a better overview of the "do's and don'ts" when it comes to assessing mitochondrial function in *Drosophila*.

Acknowledgements

We thank Rebecca Finlay for her help with fly husbandry.

Funding

This research was funded by the BBSRC (BB/S003681/1) grant to ER, SI and NL, and by the European Union's Horizon 2020 research and innovation programme under the Marie Skłodowska-Curie grant agreement No 101030803 to S.B.

References

Andreazza S, Samstag CL, Sanchez-Martinez A, Fernandez-Vizarra E, Gomez-Duran A, Lee JJ et al (2019) Mitochondrially-targeted APOBEC1 is a potent mtDNA mutator affecting mitochondrial function and organismal fitness in *Drosophila*. https://doi.org/10.1038/s41467-019-10857-y

Baggio F, Bratic A, Mourier A, Kauppila TES, Tain LS, Kukat C et al (2014) *Drosophila melanogaster* LRPPRC2 is involved in coordination of mitochondrial translation. https://doi.org/10.1093/nar/gku1132

Baker M (2016) 1,500 scientists lift the lid on reproducibility. https://doi.org/10.1038/533452a

Brandt T, Mourier A, Tain LS, Partridge L, Larsson N-G, Kühlbrandt W (2017) Changes of mitochondrial ultrastructure and function during ageing in mice and *Drosophila*. https://doi.org/10.7554/eLife.24662

Bratic A, Clemente P, Calvo-Garrido J, Maffezzini C, Felser A, Wibom R et al (2016) Mitochondrial polyadenylation is a one-step process required for mRNA integrity and tRNA maturation. https://doi.org/10.1371/journal.pgen.1006028

Bratic A, Kauppila TES, Macao B, Grönke S, Siibak T, Stewart JB et al (2015) Complementation between polymerase- and exonuclease-deficient mitochondrial DNA polymerase mutants in genomically engineered flies. https://doi.org/10.1038/ncomms9808

Bratic A, Wredenberg A, Grönke S, Stewart JB, Mourier A, Ruzzenente B et al (2011) The bicoid stability factor controls polyadenylation and expression of specific mitochondrial mRNAs in *Drosophila melanogaster*. https://doi.org/10.1371/journal.pgen.1002324

Camus MF, Clancy David J, Dowling Damian K (2012) Mitochondria, maternal inheritance, and male sging. https://doi.org/10.1016/j.cub.2012.07.018

Camus MF, Rodriguez E, Kotiadis V, Carter H, Lane N (2023) Redox stress shortens lifespan through suppression of respiratory Complex I in flies with mitonuclear incompatibilities. https://doi.org/10.1016/j.exger.2023.112158

Cardoso LHD, Doerrier C, Gnaiger E (2021) Magnesium Green for fluorometric measurement of ATP production does not interfere with mitochondrial respiration. https://doi.org/10.26124/bec:2021-0001

Carnegie L, Reuter M, Fowler K, Lane N, Camus MF (2021) Mother's curse is pervasive across a large mitonuclear *Drosophila* panel. https://doi.org/10.1002/evl3.221

Champigny C, Cormier R, Simard C, St-Coeur P-D, Fortin S, Pichaud N (2018) Omega-3 monoacylglyceride effects on longevity, mitochondrial metabolism and oxidative stress: Insights from *Drosophila melanogaster*. https://doi.org/10.3390/md16110453

Cormier RJ, Strang R, Menail H, Touaibia M, Pichaud N (2021) Systemic and mitochondrial effects of metabolic inflexibility induced by high fat diet in *Drosophila melanogaster*. https://doi.org/10.1016/j.ibmb.2021.103556

Cormier RPJ, Champigny CM, Simard CJ, St-Coeur P-D, Pichaud N (2019) Dynamic mitochondrial responses to a high-fat diet in *Drosophila melanogaster*. https://doi.org/10.1038/s41598-018-36060-5

Correa CC, Aw WC, Melvin RG, Pichaud N, Ballard JWO (2012) Mitochondrial DNA variants influence mitochondrial bioenergetics in *Drosophila melanogaster*. https://doi.org/10.1016/j.mito.2012.06.005

Costa AC, Loh SHY, Martins LM (2013) *Drosophila Trap1* protects against mitochondrial dysfunction in a PINK1/parkin model of Parkinson's disease. https://doi.org/10.1038/cddis.2012.205

Cruz LC, Ecker A, Rodrigues NR, Martins IK, Posser T, Maciel FE et al (2018) Honey protects against wings posture error and molecular changes related to mitochondrial pathways induced by hypoxia/reoxygenation in adult *Drosophila melanogaster*. https://doi.org/10.1016/j.cbi.2018.06.033

De Carvalho NR, Rodrigues NR, Macedo GE, Bristot IJ, Boligon AA, De Campos MM et al (2017) Eugenia uniflora leaf essential oil promotes mitochondrial dysfunction in *Drosophila melanogaster* through the inhibition of oxidative phosphorylation. https://doi.org/10.1039/c7tx00072c

De Castro IP, Costa AC, Celardo I, Tufi R, Dinsdale D, Loh SHY et al (2013) *Drosophila ref(2)P* is required for the *parkin*-mediated suppression of mitochondrial dysfunction in *pink1* mutants. https://doi.org/10.1038/cddis.2013.394

Doerrier C, Draxl A, Wiethuechter A, Eigentler A, Gnaiger E (2015) Mitochondrial respiration in permeabilized fibers versus homogenate from fish liver and heart. An application study with the PBI-Shredder. https://wiki.oroboros.at/index.php/MiPNet17.03_Shredder_vs_Fibers

Doerrier C, Garcia-Souza LF, Krumschnabel G, Wohlfarter Y, Mészáros AT, Gnaiger E (2018) High-Resolution FluoRespirometry and OXPHOS protocols for human cells, permeabilized fibers from small biopsies of muscle, and isolated mitochondria. https://doi.org/10.1007/978-1-4939-7831-1_3

Ebanks B, Wang Y, Katyal G, Sargent C, Ingram TL, Bowman A et al (2021) Exercising *D. melanogaster* modulates the mitochondrial proteome and physiology. The effect on lifespan depends upon age and sex. https://doi.org/10.3390/ijms222111606

Ederer KA, Jin K, Bouslog S, Wang L, Gorman GS, Rowe GC et al (2018) Age- and genotype-specific effects of the angiotensin-converting enzyme inhibitor Lisinopril on mitochondrial and metabolic parameters in *Drosophila melanogaster*. https://doi.org/10.3390/ijms19113351

Eigentler A, Draxl A, Fontana-Ayoub M, Gnaiger E (2015) Tissue homogenates for diagnosis of mitochondrial respiratory function: Mouse heart, brain and liver. https://wiki.oroboros.at/index.php/MiPNet17.15_PBI-Shredder_Mouse-heart-brain-liver

Garrido-Maraver J, Celardo I, Costa AC, Lehmann S, Loh SHY, Martins LM (2019) Enhancing folic acid metabolism suppresses defects associated with loss of *Drosophila* mitofusin. https://doi.org/10.1038/s41419-019-1496-2

Gaviraghi A, Aveiro Y, Carvalho SS, Rosa RS, Oliveira MP, Oliveira MF (2021) Mechanical permeabilization as a new method for assessment of mitochondrial function in insect tissues. https://doi.org/10.1007/978-1-0716-1266-8_5

Gnaiger E (2020) Mitochondrial pathways and respiratory control. An introduction to OXPHOS analysis. 5th ed. . https://doi.org/10.26124/bec:2020-0002

Gnaiger E (2019) Editorial: A vision on preprints for mitochondrial physiology and bioenergetics. https://doi.org/10.26124/mitofit:190002.v2

Gnaiger E - MitoEAGLE Task Group (2020) Mitochondrial physiology. https://doi.org/10.26124/bec:2020-0001.v1

Gnaiger E, Komlódi T, Schmitt S, Cecatto C, Gradl L, Gradl P (2021) O2k-FluoRespirometer manual. https://wiki.oroboros.at/index.php/MiPNet22.11_O2k-FluoRespirometer_manual

Guitart T, Leon Bernardo T, Sagalés J, Stratmann T, Bernués J, Ribas De Pouplana L (2010) New aminoacyl-tRNA synthetase-like protein in Insecta with an essential mitochondrial function. https://doi.org/10.1074/jbc.m110.167486

Guitart T, Picchioni D, Piñeyro D, Ribas De Pouplana L (2013) Human mitochondrial disease-like symptoms caused by a reduced tRNA aminoacylation activity in flies. https://doi.org/10.1093/nar/gkt402

Gururaja Rao S, Bednarczyk P, Towheed A, Shah K, Karekar P, Ponnalagu D et al (2019) BK_{Ca} (*Slo*) channel regulates mitochondrial function and lifespan in *Drosophila melanogaster*. https://doi.org/10.3390/cells8090945

Jørgensen LB, Overgaard J, Hunter-Manseau F, Pichaud N (2021) Dramatic changes in mitochondrial substrate use at critically high temperatures: a comparative study using *Drosophila*. https://doi.org/10.1242/jeb.240960

Kanellopoulos AK, Mariano V, Spinazzi M, Woo YJ, McLean C, Pech U et al (2020) Aralar sequesters GABA into hyperactive mitochondria, causing social behavior deficits. https://doi.org/10.1016/j.cell.2020.02.044

Kemppainen KK, Rinne J, Sriram A, Lakanmaa M, Zeb A, Tuomela T et al (2014) Expression of alternative oxidase in *Drosophila* ameliorates diverse phenotypes due to cytochrome oxidase deficiency. https://doi.org/10.1093/hmg/ddt601

Kuznetsov AV, Veksler V, Gellerich FN, Saks V, Margreiter R, Kunz WS (2008) Analysis of mitochondrial function in situ in permeabilized muscle fibers, tissues and cells. https://doi.org/10.1038/nprot.2008.61

Lehmann S, Loh SHY, Martins LM (2017) Enhancing NAD+ salvage metabolism is neuroprotective in a PINK1 model of Parkinson's disease. https://doi.org/10.1242/bio.022186

Li Puma L, Hedges M, Heckman JM, Mathias AB, Engstrom MR, Brown AB et al (2020) Experimental oxygen concentration influences rates of mitochondrial hydrogen peroxide release from cardiac and skeletal muscle preparations. https://doi.org/10.1152/ajpregu.00227.2019

Liu M, Yu S, Wang J, Qiao J, Liu Y, Wang S et al (2020) Ginseng protein protects against mitochondrial dysfunction and neurodegeneration by inducing mitochondrial unfolded protein response in *Drosophila melanogaster* PINK1 model of Parkinson's disease. https://doi.org/10.1016/j.jep.2019.112213

Macchi M, El Fissi N, Tufi R, Bentobji M, Liévens J-C, Martins LM et al (2012) The *Drosophila* inner-membrane protein PMI controls cristae biogenesis and mitochondrial diameter. https://doi.org/10.1242/jcs.115675

Maddison DC, Alfonso-Núñez M, Swaih AM, Breda C, Campesan S, Allcock N et al (2020) A novel role for kynurenine 3-monooxygenase in mitochondrial dynamics. https://doi.org/10.1371/journal.pgen.1009129

Markow TA (2015) The secret lives of *Drosophila* flies. https://doi.org/10.7554/elife.06793

Menail HA, Cormier SB, Ben Youssef M, Jørgensen LB, Vickruck JL, Morin P et al (2022) Flexible thermal sensitivity of mitochondrial oxygen consumption and substrate oxidation in flying insect species. https://doi.org/10.3389/fphys.2022.897174

Morrow EH (2015) The evolution of sex differences in disease. https://doi.org/10.1186/s13293-015-0023-0

Munro D, Treberg JR (2017) A radical shift in perspective: mitochondria as regulators of reactive oxygen species. https://doi.org/10.1242/jeb.132142

Oroboros-Ecosystem. O2k-Publications: Drosophila. 2023; Available from: https://wiki.oroboros.at/index.php/O2k-Publications:_Drosophila.

Oroboros-Ecosystem. Permeabilized muscle fibers. 2016; Available from: https://wiki.oroboros.at/index.php/Permeabilized_muscle_fibers.

Pajak A, Laine I, Clemente P, El-Fissi N, Schober FA, Maffezzini C et al (2019) Defects of mitochondrial RNA turnover lead to the accumulation of double-stranded RNA in vivo. https://doi.org/10.1371/journal.pgen.1008240

Pecinová A, Drahota Z, Nůsková H, Pecina P, Houštěk J (2011) Evaluation of basic mitochondrial functions using rat tissue homogenates. https://doi.org/10.1016/j.mito.2011.05.006

Pesta D, Gnaiger E (2015) Preparation of permeabilized muscle fibers for diagnosis of mitochondrial respiratory function. https://wiki.oroboros.at/index.php/MiPNet14.14_PermeabilizedFiberPreparation

Pesta D, Gnaiger E (2012) High-resolution respirometry: OXPHOS protocols for human cells and permeabilized fibers from small biopsies of human muscle. https://doi.org/10.1007/978-1-61779-382-0_3

Pichaud N, Ballard JWO, Tanguay RM, Blier PU (2012) Naturally occurring mitochondrial dna haplotypes exhibit metabolic differences: Insight into functional properties of mitochondria. https://doi.org/10.1111/j.1558-5646.2012.01683.x

Pichaud N, Ballard JWO, Tanguay RM, Blier PU (2011) Thermal sensitivity of mitochondrial functions in permeabilized muscle fibers from two populations of *Drosophila* simulans with divergent mitotypes. https://doi.org/10.1152/ajpregu.00542.2010

Pichaud N, Chatelain EH, Ballard JWO, Tanguay R, Morrow G, Blier PU. (2010) Thermal sensitivity of mitochondrial metabolism in two distinct mitotypes of Drosophila simulans: evaluation of mitochondrial plasticity. https://doi.org/10.1242/jeb.040261

Pimenta De Castro I, Costa AC, Lam D, Tufi R, Fedele V, Moisoi N et al (2012) Genetic analysis of mitochondrial protein misfolding in *Drosophila melanogaster*. https://doi.org/10.1038/cdd.2012.5

Quéméneur J-B, Danion M, Cabon J, Collet S, Zambonino-Infante J-L, Salin K (2022) The relationships between growth rate and mitochondrial metabolism varies over time. https://doi.org/10.1038/s41598-022-20428-9

Rana A, Oliveira MP, Khamoui AV, Aparicio R, Rera M, Rossiter HB et al (2017) Promoting Drp1-mediated mitochondrial fission in midlife prolongs healthy lifespan of *Drosophila melanogaster*. https://doi.org/10.1038/s41467-017-00525-4

Rodrigues APC, Camargo AF, Andjelković A, Jacobs HT, Oliveira MT (2018) Developmental arrest in *Drosophila melanogaster* caused by mitochondrial DNA replication defects cannot be rescued by the alternative oxidase. https://doi.org/10.1038/s41598-018-29150-x

Rodrigues NR, Macedo GE, Martins IK, Gomes KK, De Carvalho NR, Posser T et al (2018) Short-term sleep deprivation with exposure to nocturnal light alters mitochondrial bioenergetics in *Drosophila*. https://doi.org/10.1016/j.freeradbiomed.2018.04.549

Rodríguez E, Grover Thomas F, Camus MF, Lane N (2021) Mitonuclear interactions produce diverging responses to mild stress in *Drosophila* larvae. https://doi.org/10.3389/fgene.2021.734255

Rovenko BM, Kubrak OI, Gospodaryov DV, Yurkevych IS, Sanz A, Lushchak OV et al (2015) Restriction of glucose and fructose causes mild oxidative stress independently of mitochondrial activity and reactive oxygen species in *Drosophila melanogaster*. https://doi.org/10.1016/j.cbpa.2015.04.012

Schober FA, Tang JX, Sergeant K, Moedas MF, Zierz CM, Moore D et al (2022) Pathogenic SLC25A26 variants impair SAH transport activity causing mitochondrial disease. https://doi.org/10.1093/hmg/ddac002

Scialò F, Sriram A, Fernández-Ayala D, Gubina N, Lõhmus M, Nelson G et al (2016) Mitochondrial ROS produced via reverse electron transport extend animal lifespan. https://doi.org/10.1016/j.cmet.2016.03.009

Scialo F, Sriram A, Stefanatos R, Sanz A (2016) Practical recommendations for the use of the GeneSwitch Gal4 System to knockdDown genes in *Drosophila melanogaster*. https://doi.org/10.1371/journal.pone.0161817

Senyilmaz D, Virtue S, Xu X, Tan CY, Griffin JL, Miller AK et al (2015) Regulation of mitochondrial morphology and function by stearoylation of TFR1. https://doi.org/10.1038/nature14601

Simard CJ, Pelletier G, Boudreau LH, Hebert-Chatelain E, Pichaud N (2018) Measurement of mitochondrial oxygen consumption in permeabilized fibers of *Drosophila* using minimal amounts of tissue. https://doi.org/10.3791/57376

Stefanatos R, Sriram A, Kiviranta E, Mohan A, Ayala V, Jacobs HT et al (2012) dj-1β regulates oxidative stress, insulin-like signaling and development in *Drosophila melanogaster*. https://doi.org/10.4161/cc.22073

Suarez RK (1998) Oxygen and the upper limits to animal design and performance. https://doi.org/10.1242/jeb.201.8.1065

Suarez RK (2000) Energy metabolism during insect flight: Biochemical design and physiological performance. https://doi.org/10.1086/318112

Syrjänen L, Valanne S, Kuuslahti M, Tuomela T, Sriram A, Sanz A et al (2015) β carbonic anhydrase is required for female fertility in *Drosophila melanogaster*. https://doi.org/10.1186/s12983-015-0111-3

Thompson K, Mai N, Oláhová M, Scialó F, Formosa LE, Stroud DA et al (2018) *OXA 1L* mutations cause mitochondrial encephalopathy and a combined oxidative phosphorylation defect. https://doi.org/10.15252/emmm.201809060

Thoral E, Roussel D, Chinopoulos C, Teulier L, Salin K (2021) Low oxygen levels can help to prevent the detrimental effect of acute warming on mitochondrial efficiency in fish. https://doi.org/10.1098/rsbl.2020.0759

Treberg JR (2021) Review: Using isolated mitochondria to investigate mitochondrial hydrogen peroxide metabolism. https://doi.org/10.1016/j.cbpb.2021.110614

Tufi R, Gandhi S, De Castro IP, Lehmann S, Angelova PR, Dinsdale D et al (2014) Enhancing nucleotide metabolism protects against mitochondrial dysfunction and neurodegeneration in a *PINK1* model of Parkinson's disease. https://doi.org/10.1038/ncb2901

Ulgherait M, Chen A, McAllister SF, Kim HX, Delventhal R, Wayne CR et al (2020) Circadian regulation of mitochondrial uncoupling and lifespan. https://doi.org/10.1038/s41467-020-15617-x

Ventura-Clapier R, Moulin M, Piquereau J, Lemaire C, Mericskay M, Veksler V et al (2017) Mitochondria: a central target for sex differences in pathologies. https://doi.org/10.1042/cs20160485

Weisz ED, Towheed A, Monyak RE, Toth MS, Wallace DC, Jongens TA (2018) Loss of *Drosophila* FMRP leads to alterations in energy metabolism and mitochondrial function. https://doi.org/10.1093/hmg/ddx387

Winwood-Smith H (2021) Metabolic responses to suboptimal macronutrient ratios in *Drosophila melanogaster*. https://doi.org/10.14264/f70e3b9

Wolff JN, Pichaud N, Camus MF, Côté G, Blier PU, Dowling DK (2016) Evolutionary implications of mitochondrial genetic variation: Mitochondrial genetic effects on OXPHOS respiration and mitochondrial quantity change with age and sex in fruit flies. https://doi.org/10.1111/jeb.12822

Wredenberg A, Lagouge M, Bratic A, Metodiev MD, Spåhr H, Mourier A et al (2013) MTERF3 Regulates Mitochondrial Ribosome Biogenesis in Invertebrates and Mammals. https://doi.org/10.1371/journal.pgen.1003178

Ziech CC, Rodrigues NR, Macedo GE, Gomes KK, Martins IK, Franco JL et al (2022) Pre-imaginal exposure to mancozeb induces morphological and behavioral deficits and oxidative damage in *Drosophila melanogaster*. https://doi.org/10.1080/01480545.2022.2069802

Zucker I, Beery AK (2010) Males still dominate animal studies. https://doi.org/10.1038/465690a

Copyright © 2023 The authors. This Open Access peer-reviewed communication is distributed under the terms of the Creative Commons Attribution License, which permits unrestricted use, distribution, and reproduction in any medium, provided the original authors and source are credited. © remains with the authors, who have granted BEC an Open Access publication license in perpetuity.

Supplement

Table S1. Effect of sex and starting oxygen saturation level over the O_2 concentration at half respiration flux (C_{50}) in permeabilized *Drosophila melanogaster* thoraces.

ID	sex	oxygen	C_{50} (µM)
1Mh	M	hyperoxia	1.057
1Fh	F	hyperoxia	0.962
2Fh	F	hyperoxia	0.863
3Fh	F	hyperoxia	0.532
2Mh	M	hyperoxia	1.231
3Mh	M	hyperoxia	1.153
4Fh	F	hyperoxia	0.590
4Mh	M	hyperoxia	0.828
5Fh	F	hyperoxia	0.733
5Mh	M	hyperoxia	0.878
6Fh	F	hyperoxia	0.445
6Mh	M	hyperoxia	0.563
1Fn	F	normoxia	0.580
1Mn	M	normoxia	0.528
2Fn	F	normoxia	0.194
2Mn	M	normoxia	0.203
3Fn	F	normoxia	0.566
3Mn	M	normoxia	0.215

LM var~sex*oxygen	*mean ± SEM*	F-normoxia	0.447 ± 0.126
		F-hyperoxia	0.687 ± 0.082
		M-normoxia	0.316 ± 0.106
		M-hyperoxia	0.952 ± 0.1
	:sex		$F = 1.4417$, $P = 0.2484$
	:oxygen		**$F = 14.02$, $P = 0.0019$ ****
	:sex:oxygen		/

Respirometry data were normalized for the maximal coupled respiration and expressed as flux control ratios (*FCR*). Factors: *'oxygen'*: hyperoxia (N = 12), normoxia (N = 6); *'sex'*: females (F, N = 9) and males (M, N = 9). The main effects of factors sex and oxygen saturation level and their interaction were inferred by means of a linear model followed by ANOVA test. The best fitting model was determined though sequential model simplification. Dashed out cells are the result of step-wise model simplification. *:sex,* main effect of sex; *:oxygen*, main effect of oxygen concentration; *:sex:oxygen*, interaction. *$p \le 0.05$; **$p \le 0.01$; ***$p \le 0.001$. Data are presented separately and also as mean ± standard error of the mean (SEM). Data refer to Figure 2B

Table S2. Impact of fluorescent probes on mitochondrial respiration in permeabilized *Drosophila melanogaster* thoraces. Respirometry data were normalized for a common internal parameter, the CI-sustained coupled respiration in absence of fluorescent probes ('Nc$_P$') and expressed as flux control ratios (*FCR*).

probe	treatment	Nc$_P$	titration 1	titration 2	titration 3	titration 4	titration 5	titration 6
AmR	ctrl	1	0.9900	0.9700	0.9700	0.9600	0.9600	0.9500
AmR	treatment	1	0.9400	0.8800	0.8400	0.8000	0.7700	0.7300
AmR	ctrl	1	0.9900	0.9700	0.9600	0.9600	0.9600	0.9600
AmR	treatment	1	0.9600	0.9100	0.8800	0.8400	0.8100	0.7900
AmR	ctrl	1	0.9800	0.9300	0.9100	0.9000	0.8900	0.8800
AmR	treatment	1	0.9200	0.8300	0.7800	0.7400	0.7100	0.6800
AmR	ctrl (mean±SEM)	1±0	0.987±0.003	0.957±0.013	0.947±0.019	0.94±0.02	0.937±0.023	0.93±0.025
	treatment (mean±SEM)	1±0	0.94±0.012	0.873±0.023	0.833±0.029	0.793±0.029	0.763±0.029	0.733±0.032
	:treatment		t = 3.8829, p = 0.0178*	t = 3.1009, p = 0.03619*	t = 3.2869, p = 0.0303*	t = 4.1576, p = 0.01417*	t = 4.651, p = 0.009654**	t = 4.8498, p = 0.008341**
	p adjusted		0.0567·	0.0606·	0.0606·	0.0567·	0.0500*	0.0500*
MgG	ctrl	1	0.9963	0.9983	0.982	0.9534	0.9363	0.925
MgG	treatment	1	0.9808	0.9721	0.9426	0.913	0.899	0.8986
MgG	ctrl	1	0.9663	0.9529	0.9319	0.94	0.9265	0.9194
MgG	treatment	1	0.9068	0.8742	0.8574	0.8423	0.8306	0.8161
MgG	ctrl	1	0.9658	0.9658	0.9484	0.9386	0.9263	0.9159
MgG	treatment	1	1	0.9601	0.9402	0.9371	0.9264	0.9141
MgG	ctrl (mean±SEM)	1±0	0.984±0.009	0.972±0.014	0.954±0.015	0.944±0.005	0.93±0.003	0.92±0.003
	treatment (mean±SEM)	1±0	0.963±0.028	0.935±0.031	0.913±0.028	0.897±0.028	0.885±0.028	0.876±0.03
	:treatment		t = 0.73529, p = 0.5029	t = 1.0953, p = 0.3349	t = 1.2859, p = 0.2679	t = 1.6137, p = 0.1819	t = 1.5471, p = 0.1967	t = 1.4358, p = 0.2244
	p adjusted		1	1	1	1	1	1
Rh123	ctrl	1	0.9769	0.9623	0.9516	0.9498	0.9431	0.9383
Rh123	treatment	1	0.9558	0.8966	0.8146	0.7216	0.6111	0.4878
Rh123	ctrl	1	0.9768	0.9602	0.9531	0.9066	0.8864	0.8492
Rh123	treatment	1	0.9582	0.8992	0.7922	0.7112	0.6186	0.493
Rh123	ctrl	1	0.9763	0.9369	0.9075	0.8709	0.8298	0.7509
Rh123	treatment	1	0.9559	0.8968	0.8148	0.7484	0.6714	0.5502
Rh123	ctrl (mean±SEM)	1±0	0.977±0	0.953±0.008	0.937±0.015	0.909±0.023	0.886±0.033	0.846±0.054
	treatment (mean±SEM)	1±0	0.957±0.001	0.898±0.001	0.807±0.008	0.727±0.011	0.634±0.019	0.51±0.02
	:treatment		t = 6.9479, p = 3.957e-05***	t = 6.7954, p = 0.002449**	t = 7.7817, p = 0.001471**	t = 7.178, p = 0.001995**	t = 6.6839, p = 0.002605**	t = 5.8204, p = 0.004339**
	p adjusted		0.00023742***	0.00798**	0.00735**	0.00798**	0.00798**	0.00798**
Saf	ctrl	1	0.998	0.991	0.9882	0.982	0.9758	0.9741
Saf	treatment	1	0.9748	0.9472	0.9144	0.8444	0.6538	0.3893
Saf	ctrl	1	0.9849	0.9684	0.9493	0.9286	0.917	0.8904
Saf	treatment	1	1.0143	0.9946	0.9684	0.8939	0.7093	0.4789
Saf	ctrl	1	1.0434	1.0485	1.0377	1.0455	1.0289	1.0512
Saf	treatment	1	0.9668	0.9402	0.8975	0.8045	0.6518	0.4219
Saf	ctrl (mean±SEM)	1±0	1.009±0.018	1.003±0.024	0.992±0.026	0.985±0.034	0.974±0.032	0.972±0.046
	treatment (mean±SEM)	1±0	0.985±0.015	0.961±0.017	0.927±0.021	0.848±0.026	0.672±0.019	0.43±0.026
	:treatment		t = 1.0196, p = 0.3656	t = 1.4307, p = 0.2258	t = 1.9487, p = 0.1231	t = 3.238, p = 0.03173*	t = 8.0802, p = 0.001275**	t = 10.165, p = 0.0005274***
	p adjusted		0.4516	0.4516	0.3693	0.12692	0.006375**	0.0031644**
TMRM	ctrl	1	1.0026	0.9952	0.9815	0.985	1.0065	0.9773
TMRM	treatment	1	0.9513	0.8678	0.7645	0.6772	0.5793	0.5116
TMRM	ctrl	1	0.9676	0.9467	0.9315	0.927	0.9277	0.905
TMRM	treatment	1	0.9455	0.8971	0.8492	0.7967	0.7429	0.6765
TMRM	ctrl	1	0.9984	0.9951	0.9877	0.9759	0.9609	0.936
TMRM	treatment	1	0.9305	0.8225	0.7088	0.6296	0.5499	0.4846
TMRM	ctrl (mean±SEM)	1±0	0.99±0.011	0.979±0.016	0.967±0.018	0.963±0.018	0.965±0.023	0.939±0.021
	treatment (mean±SEM)	1±0	0.942±0.006	0.862±0.022	0.774±0.041	0.701±0.05	0.624±0.06	0.558±0.06
	:treatment		t = 3.7219, p = 0.02044*	t = 4.3081, p = 0.01257*	t = 4.3286, p = 0.01236*	t = 4.9458, p = 0.007784**	t = 5.3087, p = 0.006052**	t = 6.0112, p = 0.003856**
	p adjusted		0.03708*	0.03708*	0.03708*	0.031136*	0.03026*	0.023136*

Probes: 'AmR': Amplex® UltraRed (N = 3; solvent: DMSO); 'MgG': Magnesium green (N = 3; solvent: H_2O); 'Rh123': Rhodamine 123 (N = 3; solvent: EtOH); 'Saf': Safranin O (N = 3; solvent: H_2O); 'TMRM': Tetramethylrhodamine methyl ester (N = 3; solvent: DMSO). Each probe was tested at different sequential concentrations: AmR ('2.5 µM', '5 µM', '7.5 µM', '10 µM', '12.5 µM' and '15 µM'); MgG: ('0.275 µM', '0.55 µM', '0.825 µM', '1.1 µM', '1.375 µM' and '1.65 µM'); Rh123: ('0.2 µM', '0.4 µM', '0.6 µM', '0.8 µM', '1.0 µM' and '1.2 µM'); Saf: ('0.5 µM', '1.0 µM', '1.5 µM', '2.0 µM', '2.5 µM' and '3.0 µM'); TMRM: ('0.5 µM', '1.0 µM', '1.5 µM', '2.0 µM', '2.5 µM' and '3.0 µM'). Parallel controls were titrated with an equal volume of each probe-specific solvent. Factor: 'treatment' ('ctrl' = control using the specific solvent, 'treatment' = probe treatment). 'Nc_P': CI-sustained coupled respiration of permeabilized tissue. The effect of probe presence (':treatment') was inferred at each titration point by means of a two samples t test. p-values were adjusted using Holm's correction for multiple testing. ·0.05 > $p \leq 0.09$; *$p \leq 0.05$; **$p \leq 0.01$; ***$p \leq 0.001$. Data are presented separately and also as mean ± standard error of the mean (SEM). Data refer to Figure 4.